Fine-grained Dynamics Representation and Stability Analysis for MMC-based Hybrid AC/DC Power Systems

Jingming Cao[1], Chaoyu Dong[2*], Qian Xiao[1], Marui Li[1], Xiaodan Yu[1], Hongjie Jia[1]
[1]School of Electrical and Information Engineering, Tianjin University, Tianjin, China
[2] Nanyang Technological University, Singapore
Tel.: +86 / 18322694146.
E-Mail: dong0120@e.ntu.edu.sg

Acknowledgements

This work was supported by the National Natural Science Foundation of China (No. 52107121), and the joint project of NSFC of China and EPSRC of UK (No. 52061635103 and EP/T021969/1).

Keywords

« Modelling», «Modular Multilevel Converters (MMC)», « State-space model», « Stability analysis ».

Abstract

The hybrid AC/DC power system is favored because of its huge energy transmission capacity and excellent steerability. However, the real system is large in scale and the inner dynamics interaction and coupling are intricate, which introduces a series of stability issues for the system operation. To investigate AC/DC interaction dynamics, an MMC-based hybrid power system model is established in the state space. The model considers the detailed dynamics of both AC and DC, and their interaction, thus it can be used for AC/DC interaction study, and offer a more precise stability assessment result than either AC power system model or MMC converter model. After the verification in MATLAB/Simulink, The interaction is studied thoroughly by the proposed model, which clearly identifies the harmonic coupling between MMC and traditional power systems. The small signal stability gaps of different systems are also compared. Case results prove that the reduced-order model can be deployed to assess stability efficiently under specific circumstances. The interaction causes extra harmonics in AC affecting the hybrid system stability.

Introduction

In order to consume sustainable energy more properly and deploy large-scale transmission more productively, the interconnection between AC and DC is important even necessary. In the future, the MTDC (Multi-Terminal DC) grids will interconnect and operate in parallel with ac systems [1]. Nevertheless, AC and DC differ in the physical behaviours, control design, and time scale. Both the AC system and the DC system need complicated control to guarantee normal work and they might also need coordination control for resource sharing. Many corresponding issues like inner dynamics interaction and control design, remain to be developed. In most cases, the AC/DC interaction is considered weak. However, some articles have declared that the mutual effect could be fierce in certain circumstances [1, 2]. Therefore, it is of interest to build the model of the entire hybrid AC/DC power system and study its dynamics, especially considering the participation of power electronic devices.

A few researches have attached the detailed hybrid AC/DC power system model issue so far. Reference [3] took the converter high-order harmonics into account, established the elaborate MTDC state-space model based on the insert index theory and modular modelling design. Reference [4] considered the equations of the MMC circuit, the control system and phase-locked loop (PLL), derived the MMC-HVDC impedance model and investigated the mechanism and damping control of high frequency resonance (HFR) occurred in HVDC project. However, both [3] and [4] simplified the AC

model too much to retain its dynamics. Reference [5] treated MMC as the equivalent generator or equivalent load and built the hybrid AC/DC power system model whereas the assumptions about MMC are too strict and the DC dynamics are ignored. Reference [1] combined the AC network model and the simple MMC model together, built the multi-terminal hybrid system model and pointed out that there existed weak coupling between asynchronous grids linked via MTDC. Reference [2] applied modal coupling theory to examine the AC/DC dynamic interactions and claimed that when a complex pole of the open-loop MTDC subsystem is close to an electromechanical oscillation mode (EOM) of concern in the open-loop AC subsystem on the complex plane, the strong interaction might be caused and the stability would be degraded.

It can be found that existing researches simplify either the AC system or DC system during the analysis, which barely reflect the accurate system dynamics. To investigate the interaction between AC and DC in the hybrid system and analyse the stability more precisely, the hybrid system model considering the fine-grained dynamics of both AC and DC is established. the physical dynamics are first summarised. Given that the real hybrid system includes many controllers to ensure the normal operation, LFC (local frequency control) and several controls in MMC are considered, and the detailed hybrid system model is derived by integrating both the physical dynamics and control dynamics. After the verification in virtue of Simulink, the model is used to study the transient interaction and stability. The results indicate that the common power and voltage might be the key factor of interaction and the hybrid system has better stability compared to the AC system in specific scenarios.

Physical dynamics in hybrid AC/DC power system

The hybrid AC/DC power system here is assumed as the combination of the AC network and the converters linked to the DC lines. The AC network is connected to the converter through the AC line and the AC network can be equivalent to one single machine. The equivalent circuit diagram is shown in Fig. 1.

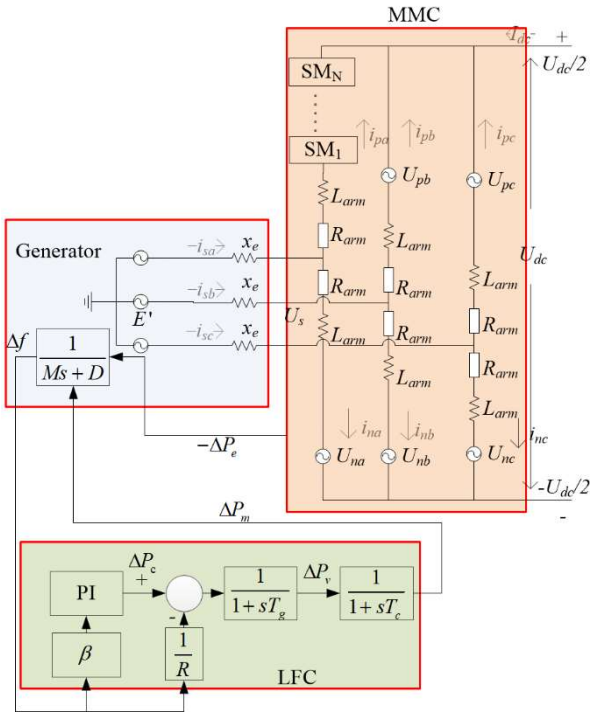

Fig. 1: The equivalent circuit diagram of the hybrid AC/DC power system.

Considering the excitation system dynamics, A fourth-order generator model [6] is deployed.

$$\Delta\dot{\delta} = 100\pi\Delta f \tag{1}$$

$$M\Delta\dot{f} = -D\Delta f + \Delta P_m - \Delta P_e \tag{2}$$

$$T_{d0}^{'}\dot{E}' = -E' + \frac{x_d - x_d^{'}}{x_e + x_d^{'}}[E' - U_s \sin(\delta)] + E_{fd} \tag{3}$$

$$T_A \dot{E}_{fd} = -K_A(U_s - U_{ref}) - (E_{fd} - E_{fd0}) \tag{4}$$

where $\Delta\delta$, Δf, ΔP_m and ΔP_e are the deviation from the power angle, frequency, mechanical power and electrical power in the equilibrium respectively. M, D, E', x_d, $x_d^{'}$ and $T_{fd0}^{'}$ are the moment of inertia, damping coefficient, transient voltage, synchronous reactance, transient reactance and transient time constant of the generator. x_e is the reactance of the AC line, U_s is the voltage of the PCC (point of common coupling) and E_{fd} is field excitation voltage. T_A and K_A are the time constant and controller gain of the excitation system. U_{ref} and E_{fd0} are the references of U_s and E_{fd} respectively.

When SM (submodule) number is big enough (for example, 250), the unbalancing effect in the different modules of a stack can be negligible and the insert index theory is considered appliable (some results in [7, 8] validated it). Based on the insert index theory, considering the harmonic dynamics in MMC, the 12th-order state-space model is presented in [7]. The AC network is connected to the converter through the AC line, thus they share the same U_s and P_e, which are the connections between them. The generator's and the converter's dynamics make up the total physical dynamics in a hybrid AC/DC power system.

However, the dynamics mentioned above are far from enough to assess the system. In practical engineering, the hybrid system is faced with the LFC need, coordination between AC and DC, and coordination among different areas, which bring the extra control dynamics to the system.

MMC-based hybrid AC/DC power system detailed state-space model

Control dynamics in hybrid AC/DC power system

The physical dynamics fail to describe the whole hybrid system, thus it's obligatory to establish a model containing both the physical dynamics and control dynamics, to study the small signal stability and transient. Frequency is a critical index of the system's safety and stable operation. According to (2), frequency is decided by the trade-off between P_m and P_e. P_m is influenced by the LFC loop and P_e equals to the power transmitted to the DC side through the converter.

The LFC loop is shown in Fig. 1, from which we derive the equations below:

$$T_{ch}\Delta\dot{P}_m = \Delta P_v - \Delta P_m \tag{5}$$

$$T_g \Delta\dot{P}_v = \Delta P_c - \Delta P_v - \Delta f / R \tag{6}$$

$$\dot{x}_{lf} = ACE = \beta\Delta f \tag{7}$$

$$\Delta P_c = -k_{plf} ACE - k_{ilf} x_{lf} = -k_{plf}\beta\Delta f - k_{ilf} x_{lf} \tag{8}$$

where ΔP_c and ΔP_v are the deviation of the PI controller output and valve position, T_g, T_{ch}, R, β and ACE are the time constant of the governor, time constant of the turbine, speed drop, frequency bias factor and the area control error. k_{plf}, k_{ilf} and x_{lf} are the proportional gain, integral gain and integrator output respectively.

PQ control, CCSC (Circulating Current Suppressing Controller) and PLL in [7] are considered in the paper. Owing to the phase adjustment of PLL, U_s becomes interrupted by the MMC and PLL dynamics. So equation (3) is rewritten as:

$$T_{d0}^{'}\dot{E}' = -E' + \frac{x_d - x_d^{'}}{x_e + x_d^{'}}[E' - U_s \sin(\delta - x_{pll})] + E_{fd} \tag{9}$$

All these MMC control dynamics may cause fluctuation of U_s and P_e, whose expressions are:

$$\begin{cases} U_{sd} = E'\sin(\delta - x_{pll}) - Ldi_{sd}/dt - \omega Li_{sq} \\ U_{sq} = E'\cos(\delta - x_{pll}) - Ldi_{sq}/dt + \omega Li_{sd} \end{cases} \tag{10}$$

$$P_e = 3(U_{sd}i_{sd} + U_{sq}i_{sq})/2 \tag{11}$$

MMC-based hybrid AC/DC power system detailed state-space model

With the physical model and the control dynamics presented above, we know that U_s and P_e in the generator model are affected by MMC. In return, MMC dynamics are relevant to δ and E' in AC. The AC system and the DC system depend on each other and can't be solved by decoupling. Thus, the hybrid system model (12) is derived by combining all the equations together:

$$\begin{bmatrix} \dot{\boldsymbol{x}}_{AC}^T & \dot{\boldsymbol{x}}_{MMC}^T & \dot{\boldsymbol{x}}_c^T \end{bmatrix}^T = \boldsymbol{f}(\boldsymbol{x}_{AC}, \boldsymbol{x}_{MMC}, \boldsymbol{x}_c, \boldsymbol{u}) \tag{12}$$

where $\boldsymbol{x}_{AC} = [E', E_{fd}, \delta, f, P_m, P_v, x_{lf}]^T$, $\boldsymbol{x}_{MMC} = [\overline{u}_c, u_c^{1d}, u_c^{1q}, u_c^{2d}, u_c^{2q}, u_c^{3x}, u_c^{3y}, I_{dc}, i_{sd}, i_{sq}, i_{cird}, i_{cirq}]^T$, $\boldsymbol{x}_c = [f_1, f_2, x_1, x_2, x_3, x_4, x_5, x_{pll}]^T$, $\boldsymbol{u} = [U_{dc}, P_{ref}, Q_{ref}, U_{ref}, E_{fd0}]^T$.

According to model (12), the AC sub-model and DC sub-model are coupled by P_e and U_s because they share the same electrical power and PCC voltage, which indicates AC and DC might have transient interaction through P_e and U_s. Considering that MMC is a typical multiple harmonic response system [9, 10], the intricate DC harmonics might affect AC and make AC's harmonic distribution complicated. After linearisation, 3 simple state-space sub-models can be obtained directly:

$$\Delta\dot{\boldsymbol{x}}_{MMC} = \boldsymbol{A}\Delta\boldsymbol{x}_{MMC} + \boldsymbol{B}\Delta\boldsymbol{u}_{MMC} \tag{13}$$

$$\Delta\dot{\boldsymbol{x}}_c = \boldsymbol{A}_c\Delta\boldsymbol{x}_c + \boldsymbol{B}_c\Delta\boldsymbol{u}_c \tag{14}$$

$$\Delta\dot{\boldsymbol{x}}_{AC} = \boldsymbol{A}_{AC}\Delta\boldsymbol{x}_{AC} + \boldsymbol{B}_{AC}\Delta\boldsymbol{u}_{sdq} + \boldsymbol{C}_{AC}\Delta\boldsymbol{x}_c \tag{15}$$

where $\Delta\boldsymbol{u}_{sdq} = [\Delta U_{sd}, \Delta U_{sq}]^T$ is linearised from (10). $\Delta\boldsymbol{u}_{MMC}$ and $\Delta\boldsymbol{u}_c$ also contain ΔU_{sd} and ΔU_{sq} terms. Therefore, even though the several sub-models can't be combined together directly, solving (16) and (17) below simultaneously to eliminate the $\Delta\boldsymbol{u}_{sdq}$ term can be an accessible approach to derive the linearised hybrid system state-space model.

$$\begin{bmatrix} \Delta\dot{\boldsymbol{x}}_{MMC} \\ \Delta\dot{\boldsymbol{x}}_c \\ \Delta\dot{\boldsymbol{x}}_{AC} \end{bmatrix} = \begin{bmatrix} \boldsymbol{A} & \boldsymbol{O} & \boldsymbol{O} \\ \boldsymbol{O} & \boldsymbol{A}_c & \boldsymbol{O} \\ \boldsymbol{O} & \boldsymbol{C}_{AC} & \boldsymbol{A}_{AC} \end{bmatrix} \begin{bmatrix} \Delta\boldsymbol{x}_{MMC} \\ \Delta\boldsymbol{x}_c \\ \Delta\boldsymbol{x}_{AC} \end{bmatrix} + \begin{bmatrix} \boldsymbol{B}_1 & \boldsymbol{B}_2 & \boldsymbol{O} & \boldsymbol{O} \\ \boldsymbol{O} & \boldsymbol{B}_{c1} & \boldsymbol{B}_{c2} & \boldsymbol{O} \\ \boldsymbol{O} & \boldsymbol{O} & & \boldsymbol{B}_{AC} \end{bmatrix} \begin{bmatrix} \Delta\boldsymbol{u}_{MMC1} \\ \Delta\boldsymbol{u}_{sdq} \\ \Delta\boldsymbol{u}_{c1} \\ \Delta\boldsymbol{u}_{sdq} \\ \Delta\boldsymbol{u}_{sdq} \end{bmatrix} \begin{matrix} \} \Delta\boldsymbol{u}_{MMC} \\ \\ \} \Delta\boldsymbol{u}_c \\ \\ \end{matrix} \tag{16}$$

$$\Delta\boldsymbol{u}_{sdq} = \boldsymbol{A}'\Delta\boldsymbol{x}_{MMC} + \boldsymbol{B}'\Delta\boldsymbol{x}_c + \boldsymbol{C}'\Delta\dot{\boldsymbol{x}}_{MMC} + \boldsymbol{D}'\Delta\boldsymbol{x}_{AC} \tag{17}$$

After daedal algebraic deduction, equation (16) becomes (18) below, denoting $\Delta\boldsymbol{x} = [\Delta\boldsymbol{x}_{MMC}^T, \Delta\boldsymbol{x}_c^T, \Delta\boldsymbol{x}_{AC}^T]^T$, $\Delta\boldsymbol{u} = [\Delta U_{dc}, \Delta P_{ref}, \Delta Q_{ref}, \Delta U_{ref}, \Delta E_{fd0}]^T$, the entire hybrid system detailed state-space model (19) is established.

$$\begin{bmatrix} \Delta\dot{\boldsymbol{x}}_{MMC} \\ \Delta\dot{\boldsymbol{x}}_{c} \\ \Delta\dot{\boldsymbol{x}}_{AC} \end{bmatrix} = \begin{bmatrix} \boldsymbol{A}_{hy}^{11} & \boldsymbol{A}_{hy}^{12} & \boldsymbol{A}_{hy}^{13} \\ \boldsymbol{A}_{hy}^{21} & \boldsymbol{A}_{hy}^{22} & \boldsymbol{A}_{hy}^{23} \\ \boldsymbol{A}_{hy}^{31} & \boldsymbol{A}_{hy}^{32} & \boldsymbol{A}_{hy}^{33} \end{bmatrix} \begin{bmatrix} \Delta\boldsymbol{x}_{MMC} \\ \Delta\boldsymbol{x}_{c} \\ \Delta\boldsymbol{x}_{AC} \end{bmatrix} + \boldsymbol{B}_{hy}[\Delta U_{dc}, \Delta P_{ref}, \Delta Q_{ref}, \Delta U_{ref}, \Delta E_{fd0}]^T \tag{18}$$

$$\Delta\dot{\boldsymbol{x}} = \boldsymbol{A}_{hy}\Delta\boldsymbol{x} + \boldsymbol{B}_{hy}\Delta\boldsymbol{u} \tag{19}$$

The differences between sub-models and the hybrid model are shown in Table I. It can be seen that the AC sub-model (15)'s dimension is much smaller than the dimension of the DC sub-model (13)+(14). DC dynamics coupling is tighter thus it has more harmonics and dimension consequently. The sub-models are integrated together through $\Delta\boldsymbol{u}_{sdq}$, forming the hybrid model (18). Nonetheless, $\boldsymbol{A}_{hy}$ doesn't equal to the block combination of $\boldsymbol{A}_{AC}$ and $\boldsymbol{A}_{DC}$. It's denser and has no zero block matrix because AC and DC have a close link due to the same input $\Delta\boldsymbol{u}_{sdq}$. It means that the model considers the physical coupling between AC and DC, and the control dynamics effect. Both AC and DC disturbances can incur the system transient process. With model (12) and model (19), we're able to assess the small signal stability and transient.

Table I: Different models comparison

Model	State variables	Input	Jacobian matrix
Sub-model (15)	$\Delta\boldsymbol{x}_{AC\ 7*1}$	$\Delta\boldsymbol{u}_{sdq}$, $\Delta\boldsymbol{x}_c$, $\Delta\boldsymbol{u}$	$\boldsymbol{A}_{AC\ 7*7}$
Sub-model (13)+(14)	$[\Delta\boldsymbol{x}_{MMC}^T, \Delta\boldsymbol{x}_c^T]_{20*1}^T$	$\Delta\boldsymbol{u}_{sdq}$, $\Delta\boldsymbol{u}$	$\boldsymbol{A}_{DC\ 20*20}$
Hybrid model (18)	$\Delta\boldsymbol{x}_{\ 27*1}$	$\Delta\boldsymbol{u}$	$\boldsymbol{A}_{hy\ 27*27}$

Model verification and modal identification

Part of the parameters of the Zhoushan multi-terminal VSC-HVDC transmission project [6, 11] are selected to verify the established model and study the hybrid system behaviours. The generator parameters are $[M, D, x_d, x_d^{'}, x_e, T_{d0}^{'}, T_A, U_{ref}, E_{fd0}, K_A]$=[10,1,1,0.4,0.5,10,10,1,1,190], base values [U_B, f_B]=[$220/\sqrt{3}$ kV, 50Hz]. The LFC parameters are presented as [T_{ch}, T_g, R, β, k_{plf}, k_{ilf}]=[0.3,0.1,0.05, 21,0.2,0.2]. As for the MMC, SM number N=250, arm inductance and resistance [L_{arm}, R_{arm}]=[0.09H, 1Ω] and SM capacitance C=6000μF. The parameters of the MMC control are: PQ control [k_{p1}, k_{i1}, k_{p2}, k_{i2}, P_{ref}, Q_{ref}]=[0.001,0.1,0.1,1,400MW,0]; CCSC [k_{p3}, k_{i3}]=[10,1000]; PLL [k_{ppll}, k_{ipll}]=[5,100].

To test the capability of the proposed model during the dynamic representation, we give P_{ref} a step change from 400MW to 420MW at t=1.8s and the time-domain responses of AC (f) and DC (i_{sd}) are given both in Simulink and the Runge-Kutta simulation (RK simulation) based on model (12). The comparison results are shown in Fig. 2. It shows that the waveforms of Simulink and the RK

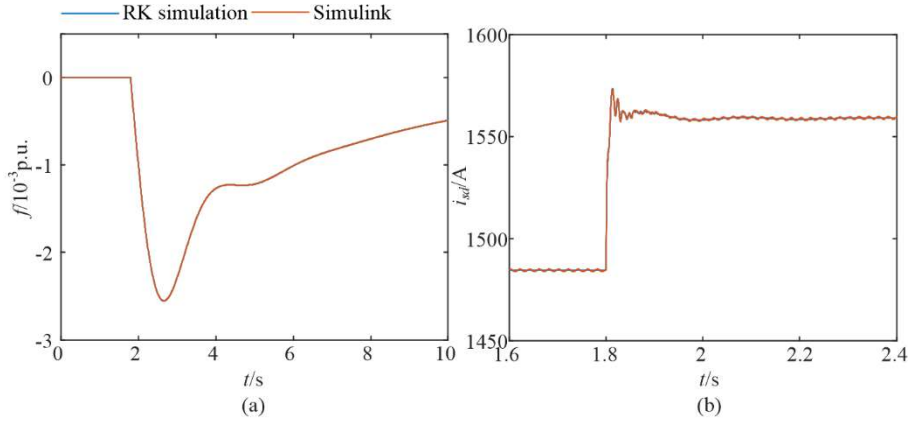

Fig. 2: The time-domain response of: (a) f, (b) i_{sd}.

simulation almost coincide, which indicates the model is able to represent system dynamics correctly.

To verify the small signal stability model (19), the eigenvalues with certain parameters varying are plotted and observed. The corresponding parameters' stability margins are compared among different approaches, which are listed in Table II. The results demonstrate the accuracy of the model (19).

Table II: Parameters margins comparison

	Simulink	RK simulation	Eigenvalues
(UM,CMF) of k_{plf}	(5.67,5.883)	(5.66,5.883)	(5.66,5.886)
(UM,CMF) of k_{ilf}	(2.54,2.501)	(2.54,2.497)	(2.54,2.498)
(LM,CMF) of M	(1.17,7.005)	(1.19,6.950)	(1.19,6.946)
UM means Upper Margin, LM means Lower Margin, CMF means Critical Mode Frequency.			

To investigate the small signal characteristics, the hybrid system eigenvalues (HSE) should be identified and classified. The eigenvalues of the hybrid system, the pure MMC system (MMC and MMC control) and the pure AC system (generator and LFC loop) are plotted and compared in Fig. 3. We can divide HSE into 3 types: b1) the ones almost coinciding with pure MMC roots; b2) the ones almost coinciding with pure AC roots; b3) the conjugate roots E1 and E2 marked in Fig. 3(c).

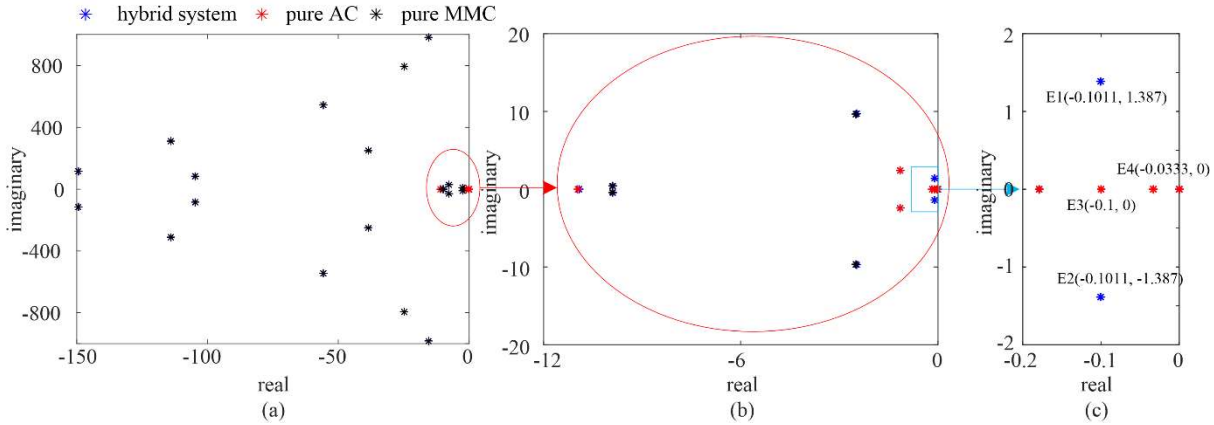

Fig. 3: The eigenvalues of the hybrid system, the pure MMC system and the pure AC system.

Among all the roots of pure AC and pure MMC, only 2 roots don't coincide with HSE, which are E3 and E4. We analysed the participate factor (PF) [3] of E3 and E4, found that they were dominated by E_{fd0} and E' respectively. In the pure AC system, E_{fd0} and E' are mainly affected by themselves, and their dynamics are not involved with oscillation. While in the hybrid system, the oscillatory U_s dynamic is considered, U_s is affected by E', E' is affected by E_{fd0} and E_{fd0} is affected by U_s. The closed-loop is formed and U_s brings the loop oscillation mode, so the real roots E3 and E4 become the conjugate roots E1 and E2 in the hybrid system. PF of E1 and E2 shown in Fig. 4 demonstrates the

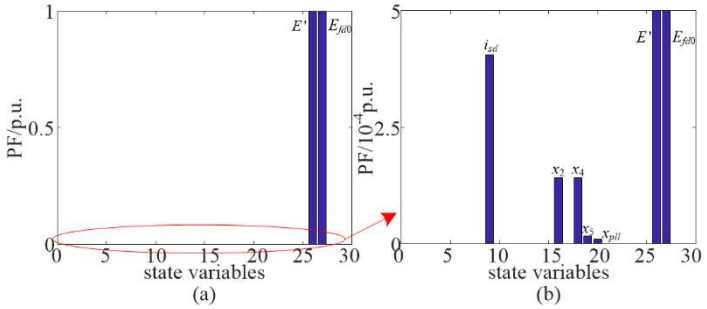

Fig. 4: The PF of E1 and E2 in the hybrid system.

mutual effect of E_{fd0} and E', and their dynamic's participation. We name b1) as DC-related roots, name b2) and b3) collectively as AC-related roots.

Hybrid system interaction investigations

We give an additional power P_{ad}=-0.2p.u. at t=1.8s to simulate part of the generator set lose connection, the DC side is affected by the AC transient and its MMC circulating current response is shown in Fig. 5(a). Once P_{ad} is exerted, f starts to deviate according to (2), then power angle will change and the power balance decided by the angle difference is broken, causing the converter couldn't transmit the wanted P_{ref}. In the meantime, PLL starts to trace the changed δ, the original dq rotating frame steady state is also broken. Thus the current increases initially. With the LFC regulation and PQ control adjustment, the power balance can be rebuilt. PLL also tends to be stable once f remains constant. Then the circulating current returns to zero under the CCSC control.

Similarly, the sub-module capacitor voltage decrement Δu_c=-150V is added at t=1.8s to simulate part of the sub-modules getting bypassed out of the fault. According to the MMC equations, It's easy to see that di_{sd}/dt increases and U_s decreases with the u_c decreases, thus P_e increases as the potential difference between the generator and the converter is reduced. So f declines at the very start. The excess power charges the capacitor to the original state and f returns to 50Hz as the power balance is reconstructed under the influence of PQ control and LFC. The frequency waveform in Fig. 5(b) coincides with the analysis above.

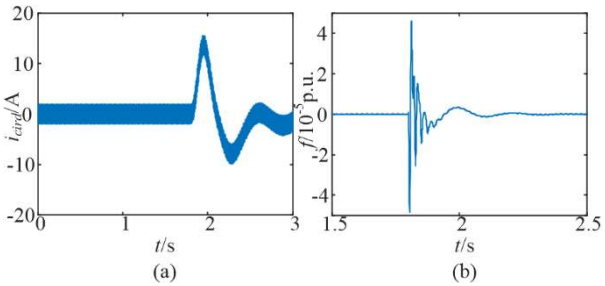

Fig. 5: The Simulink time-domain response of: (a) i_{cird}, (b) f.

To distinguish the differences between the traditional power system and the hybrid system, assume 2 cases: a1) traditional case in which the generator connects with AC load directly; a2) hybrid case that the generator is linked to the equal-sized DC load through the MMC converter. We sample and observe the harmonic components of the transmitted current i_{sd} after the system startup. The sampled harmonics are shown in Fig. 6 which is plotted with the aid of FFT Analysis. Apparently, harmonics of a2) are far bigger than harmonics of a1). And a2) has distinct components that a1) does not have, in f=150Hz and f=300Hz. Other than the fundamental, the biggest current component is of 5 orders (the 3-order component is eliminated). After the Park transformation, it will turn to the peak whose f=300Hz (and a small f=200Hz peak). As for another peak, MMC introduces the even-order circulating current inevitably. The biggest component is of 4 orders since the 2-order current is suppressed by CCSC. Likewise, it becomes an f=150Hz peak and a small f=250Hz peak. With the corresponding analysis and histograms, we know that the hybrid system has more abundant harmonics than the traditional system owing to its DC part.

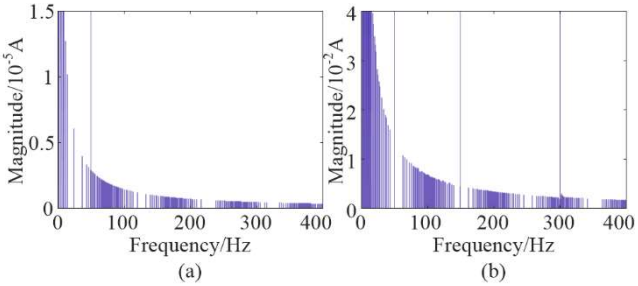

Fig. 6: Harmonic histogram: (a) traditional AC, (b) hybrid AC/DC system.

The researches above testify the indication, that AC and DC have transient interaction through P_e and U_s mutually indeed. Also the results show that the established model is able to reflect the transient interaction between AC and DC.

The root locus with M varying and the root locus with k_{il} varying are plotted in Fig. 7 and Fig. 8. It can be seen that DC-related roots seldom move when M varies and AC-related roots seldom move when k_{il} varies. Unlike notable transient change, the small signal disturbance might be insufficient to affect the other side through power or voltage directly.

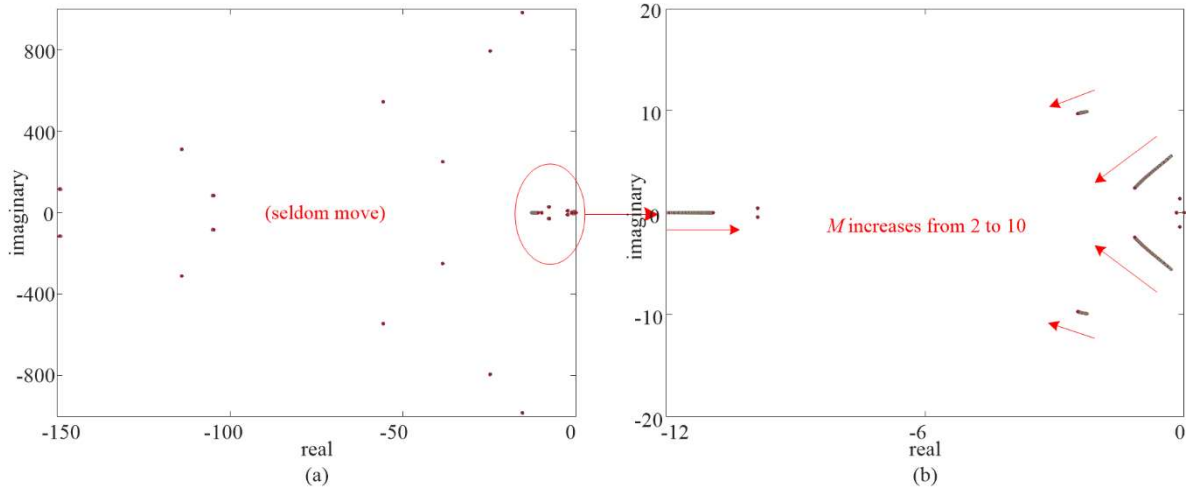

Fig. 7: The root locus when M increases from 2 to 10.

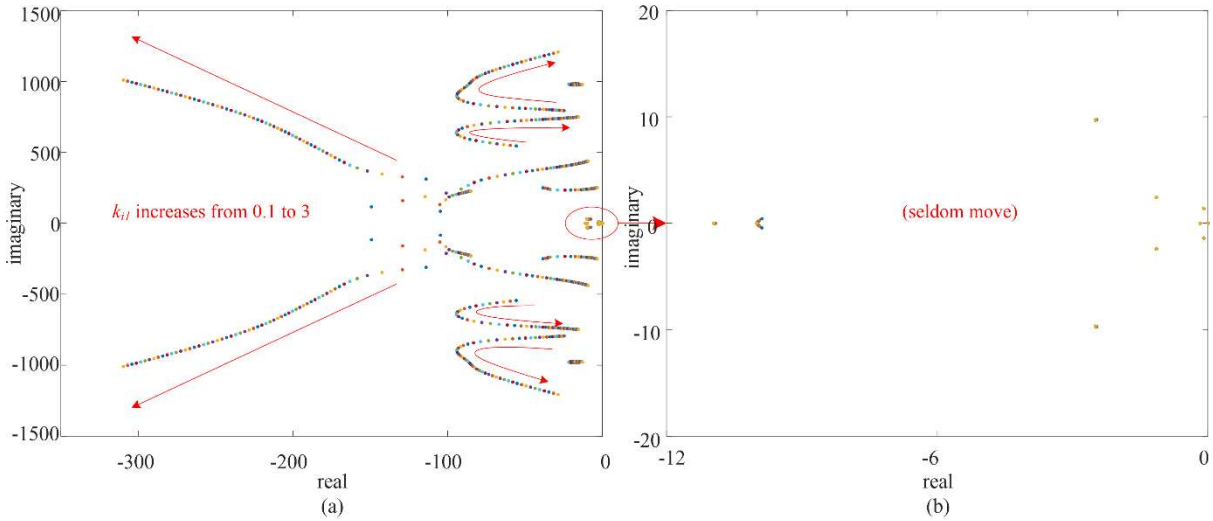

Fig. 8: The root locus when k_{il} increases from 0.1 to 3.

As for the stability margins comparison among the hybrid system, the pure MMC system and the pure AC system, the obtained results reflect that the hybrid system has almost the same margins as the pure MMC system. As the AC time scale is much larger than the DC time scale, from DC's view, the AC side changes so slow that it can be regarded as fixed. AC dynamics do no contribution to the DC small signal stability, leading to the same margins with pure MMC system. With this conclusion, deploying the reduced-order MMC model to study the DC-side stability might be a more efficient idea.

On the other side, however, we found that compared to the pure AC system, the hybrid system has larger AC parameters margins. The comparison whose data are calculated and checked by the RK simulation and eigenvalues is listed in Table III. Contrast to the pure AC system's constant PCC voltage situation, the hybrid system's PCC voltage is affected by the converter's fast response. Under

the PQ control effect, the converter response helps to maintain power within a certain range in most cases, thus the hybrid system has better AC-side stability due to the DC's fast regulation.

Table III: AC and hybrid system margins comparison

	(UM,CMF) of k_{plf}	(UM,CMF) of k_{ilf}	(LM,CMF) of M
AC system	(5.57,5.851)	(2.53,2.499)	(1.51,6.303)
MMC-based Hybrid system	(5.66,5.883)	(2.54,2.497)	(1.19,6.950)

Conclusion

The physical dynamics in hybrid AC/DC power systems are modelled with a generator model and MMC state-space model based on the insert index theory. Taking load frequency control and MMC control into consideration, the detailed hybrid system model is derived by integrating both the physical dynamics and control dynamics. The established model is verified with Simulink and parameter stability margins. After the elaborate investigation, 5 key conclusions are drawn:

c1) The established model is able to reflect the system transient and small signal dynamics accurately, which is competent for the quantitative study on hybrid AC/DC power system stability.

c2) In the hybrid system, AC and DC interact through P_e and U_s. The interaction might be more intense once one part breaks down, so applying the built model to study the hybrid system transient issue is of great significance.

c3) The change brought by AC/DC interaction strengthens the coupling between the roots dominated by E_{fd0} and E' and turns them into a pair of conjugate roots.

c4) AC dynamics barely affect the DC small signal stability due to the time scale difference. Hence, the reduced-order MMC model instead of the whole hybrid system model is more efficient to study DC-side stability.

c5) The hybrid system has better AC-side stability due to the DC's fast regulation, which confirms that the paper's meticulous hybrid system modelling is worthwhile.

References

[1] A. G. Endegnanew, G. Bergna-Diaz and K. Uhlen, "Avoiding AC/DC grid interaction in MMC based MTDC systems," in 2017 Twelfth International Conference on Ecological Vehicles and Renewable Energies (EVER), 2017, pp. 1-8.

[2] W. Du, Q. Fu and H. Wang, "Strong dynamic interactions between multi‐terminal DC network and AC power systems caused by open-loop modal coupling," IET Generation, Transmission & Distribution, vol. 11, pp. 2362-2374, 2017.

[3] J. Cao, C. Dong, Q. Xiao, X. Yu, and H. Jia, "State Modeling and Stability Analysis of the Multi-terminal MMC-HVDC Cyber-physical System Considering the Control and Communication Delay," Proceedings of the CSEE, vol. 41, pp. 3547-3560, 2021(in Chinese).

[4] Y. Li, T. An, D. Zhang, X. Pei, K. Ji, and G. Tang, "Analysis and Suppression Control of High Frequency Resonance for MMC-HVDC System," IEEE Transactions on Power Delivery, vol. 36, pp. 3867-3881, 2021.

[5] Y. Liu, Z. Lin, K. Xiahou, Y. Lin, and Q. H. Wu, "Equivalent hamiltonian equations modelling and energy function construction for MMC-HVDC in hybrid AC/DC power systems," CSEE Journal of Power and Energy Systems, vol. 7, pp. 821-831, 2021.

[6] H. Jia, J. Chen, and X. Yu, "Impact of Delay on Power System Small Signal Stability," Automation of Electrical Power System, vol. 30, pp. 5-8, 2006(in Chinese).

[7] T. Li, A. M. Gole and C. Zhao, "Small-Signal Model of the Modular Multilevel Converter Considering the Internal Dynamics," Proceedings of the CSEE, vol. 36, pp. 2890-2899, 2016(in Chinese).

[8] T. Li, A. M. Gole and C. Zhao, "Harmonic Instability in MMC-HVDC Converters Resulting From Internal Dynamics," IEEE Transactions on Power Delivery, vol. 31, pp. 1738-1747, 2016.

[9] K. Ji, G. Tang, J. Yang, Y. Li, and D. Liu, "Harmonic Stability Analysis of MMC-Based DC System Using DC Impedance Model," IEEE Journal of Emerging and Selected Topics in Power Electronics, vol. 8, pp. 1152-1163, 2020.

[10] J. Cao, C. Dong, X. Yu, R. Wang, Q. Xiao, and H. Jia, "Modelling and stability assessment of the MMC - HVDC energy interconnected system with the cyber delay of communication network," IET Energy Systems Integration, vol. 3, pp. 86-98, 2021.

[11] L. Liu, X. Cai, E. Yu, and X. Yu, "Zhoushan Multi-Terminal VSC-HVDC Transmission Demonstration Project and Its Evaluation," Southern Power System Technology, vol. 13, pp. 79-88, 2019(in Chinese).